Seismoelectric waves in a borehole excited by an external explosive source*

Zhou Jiu-Guang(周久光)[a)b)], Cui Zhi-Wen(崔志文)[a)†], Lü Wei-Guo(吕伟国)[a)], Zhang Yu-Jun(张玉君)[a)], and Wang Ke-Xie(王克协)[a)]

[a)] College of Physics, Jilin University, Changchun 130012, China
[b)] School of Basic Medical, Beihua University, Jilin 132001, China

(Received 24 January 2013; revised manuscript received 27 March 2013; published 2 December 2013)

The conversion of energy between seismic and electromagnetic wave fields has been described by Pride's coupled equations in porous media. In this paper, the seismoelectric field excited by the explosive point source located at the outside of the borehole is studied. The scattering fields inside and outside a borehole are analyzed and deduced under the boundary conditions at the interface between fluid and porous media. The influences of the distance of the point source, multipole components of the eccentric explosive source, and the receiving position along the axis of vertical borehole, on the converted waves inside the borehole are all investigated. When the distance from the acoustic source to the axis of a borehole is far enough, the longitudinal and coseismic longitudinal wave packets dominate the acoustic and electric field, respectively. The three components of both electric field and magnetic field can be detected, and the radial electric field is mainly excited and converted by the dipole component. Owing to the existence of borehole, the electric fields and magnetic fields in the borehole are azimuthal. The distance from the point where the maximum amplitude of the axial components of electric field is recorded, to the origin of coordinate indicates the horizontal distance from the explosive source to the axis of vertical borehole.

Keywords: poroelastic wave, borehole, scattering field, explosive source

PACS: 43.20.+g, 91.60.Lj, 91.30.–f **DOI:** 10.1088/1674-1056/23/1/014301

1. Introduction

Grain surfaces in contact with an electrolyte adsorb a chemically bound surface charge that is balanced by mobile counter ions in a thin fluid layer surrounding the grains. The ensemble of bound and mobile charge layers is referred to as the electric double layer.[1] Thus, a seismic wave that travels through a porous medium induces the pore fluid motion. The fluid motion with respect to the charge bound to the grain surface transports the mobile counter ions in the double layer and generates an electric wave current on the scale of the wavelength. In brief, the seismoelectric effect is the coupling between the elastic wave fields and the electromagnetic fields in the range of seismic frequencies.

For a fluid-saturated porous medium, we can distinguish two kinds of seismoelectric effects. (1) Inside a homogeneous porous medium, a coseismic electric field is coupled to a seismic wave and therefore propagates with seismic wave velocity.[2] The coseismic magnetic fields associated with a Stoneley wave[3] and a shear wave have been measured.[4,5] (2) At an interface between two distinct porous media, a seismic wave induces a radiating electromagnetic (EM) wave that can be received synchronously at multilocations.[2,6] These effects have been verified experimentally in the laboratory[7–10] and in the field.[11–17]

Seismoelectric imaging can combine the high-spatial-resolution seismic data with the sensitivities of electrical method to fluid content, connectivity, and composition. Seismoelectric investigations have been made to image the subsurface, and also to locate potential oil and gas reservoirs.[18] Especially the method of acoustoelectric well logging in porous media has been proposed to detect deep target formation. There have been many numerical simulations[19–23] and experiments[3,7,8,24–27] on the seismoelectric effect that the acoustic source located inside a borehole, especially the non-axisymmetric acousto-electric field excited by an eccentric acoustic source in the borehole, was considered by Cui *et al.*[23] In the above case, the incident field was the only acoustic wave field excited by an acoustic source located in the borehole. In order to survey cross borehole, several well-known experiments were performed by Zhu and Toksöz,[9] and Araji *et al.*[28] proposed a cross-hole imaging approach (for obtaining compact volumetric current source distributions) based on seismoelectric conversions.[28] In such a case, the seismoelectric coupling effect between the incident acoustic wave field and the shooting borehole needs to be considered. Moreover, Gao and Hu[29] studied the properties of seismoelectromagnetic waves radiated by a double couple in the porous for-

*Project supported by the National Natural Science Foundation of China (Grant Nos. 40974067, 11134011, and 41004044), the State Key Laboratory of Acoustics, Chinese Academy of Sciences (Grant No. SKLOA201108), and the Scientific Forefront and Interdisciplinary Innovation Project of Jilin University, China.

†Corresponding author. E-mail: cuizw@jlu.edu.cn

© 2014 Chinese Physical Society and IOP Publishing Ltd

mation, and they also[30] investigated the surface electromagnetic wavefields generated by a finite fault. To the best of our knowledge, an insightful understanding of acoustoelectric field characteristics which are excited and converted by the acoustic source outside the borehole, is lacking at present. In the present paper, we will focus on the non-axisymmetric acoustic-electric field excited by an eccentric acoustic source outside of the borehole. We theoretically formulate and numerically simulate the seismoelectric field in a fluid-filled borehole. The full waveforms of acoustic waves and electromagnetic waves propagating in the borehole are simulated and investigated.

2. Model and theory

2.1. Physical model

Physical model is shown in Fig. 1, a point source is located at (r_0, θ_0, 0) outside the borehole in a cylindrical coordinate system, and the z axis is coincident with the axis of vertical borehole. Here, r_0 is the distance from the point source to the axis of coordinate, θ_0 is the inclined angle, i.e., the off-x-axis angle of the source. The receiving devices are located at position ($r_{\rm re}$, θ, z) inside the borehole, with $r_{\rm re}$ being the distance from the receivers to the z axis, and θ being the angle of the receivers relative to the x axis.

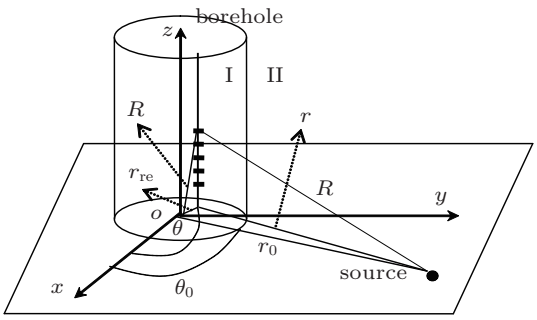


Fig. 1. Physical model.

2.2. Seismoelectric waves in the saturated porous medium

According to Pride's theory, in the absence of the applied force and electric current sources, we may write the equations for the coupled electromagnetic and acoustic fields in fluid saturated porous medium as follows:

$$\nabla \times \boldsymbol{E} = \mathrm{i}\omega \boldsymbol{B}, \tag{1a}$$

$$\nabla \times \boldsymbol{H} = \mathrm{i}\omega \boldsymbol{D} + \boldsymbol{J}, \tag{1b}$$

$$\nabla \cdot \boldsymbol{\tau} = -\omega^2(\rho \boldsymbol{u} + \rho_{\rm f} \boldsymbol{w}), \tag{1c}$$

$$\boldsymbol{J} = \sigma(\omega)\boldsymbol{E} + L(\omega)(-\nabla p + \omega^2 \rho_{\rm f} \boldsymbol{u}), \tag{1d}$$

$$-\mathrm{i}\omega \boldsymbol{w} = L\boldsymbol{E} + (-\nabla p + \omega^2 \rho_{\rm f} \boldsymbol{u})\kappa(\omega)/\eta, \tag{1e}$$

$$\boldsymbol{\tau} = (H - 2G)(\nabla \cdot \boldsymbol{u})\boldsymbol{I} + C(\nabla \cdot \boldsymbol{w})\boldsymbol{I} + G(\nabla \boldsymbol{u} + \nabla \boldsymbol{u}^{\rm T}), \tag{1f}$$

$$-p = C\nabla \cdot \boldsymbol{u} + M\nabla \cdot \boldsymbol{w}, \tag{1g}$$

$$\boldsymbol{B} = \mu \boldsymbol{H}, \tag{1h}$$

$$\boldsymbol{D} = \varepsilon \boldsymbol{E}. \tag{1i}$$

These governing equations are the Biot equations for porous medium acoustics along with the Maxwell equations for the electric and magnetic fields $\boldsymbol{E}$ and $\boldsymbol{H}$. Here, $\boldsymbol{\tau}$ is the bulk stress in the porous medium, p is the pressure in the pore fluid, $\boldsymbol{u}$ is the displacement in the solid, and $\boldsymbol{w}$ is the relative fluid–solid motion. The symbol ρ denotes the bulk density of the porous medium. The fourth and fifth equations are in the form of Darcy law and Ohm's law, through which acoustic and electromagnetic fields are coupled. Here, $\boldsymbol{J}$ is the electric-current density; $-\mathrm{i}\omega \boldsymbol{w}$ is the Darcy filtration velocity; H, C, M, and G are four moduli of isotropic porous medium; ε is the permittivity of porous medium; $\sigma(\omega)$ is the frequency-dependent electrical conductivity of the medium; $\kappa(\omega)$ is the dynamic permeability; η is the fluid dynamic viscosity coefficient; $L(\omega)$ is the frequency-dependent electrokinetic coupling coefficient. The expressions for $\sigma(\omega)$, $k(\omega)$, and $L(\omega)$ are given in Refs. [1], [2], and [6].

We decompose basic vector fields $\boldsymbol{u}$, $\boldsymbol{w}$, and $\boldsymbol{E}$ into their compressional, vertically and horizontally polarized shear components, and further express them in terms of scalar potential functions which can be found in Ref. [22].

$$\begin{aligned}\boldsymbol{u}^{(\rm r)} &= \left(\sum \nabla \varphi_j\right)_{j=\rm pf,ps} + \left(\sum \nabla \times (\chi_j e_z)\right)_{j=\rm sh,te} \\ &\quad + \left(\sum \nabla \times \nabla \times (\Gamma_j e_z)\right)_{j=\rm sv,tm}, \end{aligned} \tag{2a}$$

$$\begin{aligned}\boldsymbol{w}^{(\rm r)} &= \left(\sum a_j \nabla \varphi_{\rm j}\right)_{j=\rm pf,ps} + \left(\sum a_j \nabla \times (\chi_j e_z)\right)_{j=\rm sh,te} \\ &\quad + \left(\sum a_j \nabla \times \nabla \times (\Gamma_j e_z)\right)_{j=\rm sv,tm}, \end{aligned} \tag{2b}$$

$$\begin{aligned}\boldsymbol{E}^{(\rm r)} &= \left(\sum \beta_j \nabla \varphi_j\right)_{j=\rm pf,ps} + \left(\sum \beta_j \nabla \times (\chi_j e_z)\right)_{j=\rm sh,te} \\ &\quad + \left(\sum \beta_j \nabla \times \nabla \times (\Gamma_{\rm j} e_z)\right)_{j=\rm sv,tm}, \end{aligned} \tag{2c}$$

where φ_j is the compressional wave potential; e_z is the unit vector in the$z$ direction; χ_j is the horizontal polarized shear potential; Γ_j is vertically polarized shear wave potential. The expressions for α_j and β_j (j = pf, ps, sh, te, sv, tm) are given in Ref. [2].

The overall seismoelectric fields outside the borehole should include the incident field produced by the acoustic source and the reflection field induced by the boundary in borehole wall.

2.2.1. Incident field in fluid-saturated porous medium

An explosive source is assumed to be located at the point (r_0, θ_0, 0), and it will radiate spherical wave with velocity $V_{\rm pf}$ in the infinite porous formation. Using the cylinder integral and Bessel function addition theorem, the displacement potential of a explosive point source in the frequency-axial-wavenumber domain can be expressed as

$$\phi^{(\rm d)}(r, \theta, k_z, \omega) = -Q\frac{F(\omega)}{2\pi}\sum_{n=0}^{\infty} \varepsilon_n K_n(\eta_{\rm pf} r_0)$$

$$\times I_n(\eta_{\rm pf} r)\cos n(\theta-\theta_0), \qquad (3)$$

where $F(\omega)$ is the Fourier transform of the acoustic source function $f(t)$; Q is the volume constant (for convenience, we set $Q=1$ m^3); ε_n is Neumann's factor ($\varepsilon_n=1$ for $n=0$; $\varepsilon_n=2$ for $n\neq 0$); $\eta_{\rm pf}$ is the radial wavenumber and $\eta_{\rm pf}^2 = k^2-\omega^2/V_{\rm pf}^2$; I_n and K_n denote the $n^{\rm th}$-order modified Bessel function of first kind and that of second kind, respectively.

It should be noted that for the convenience of discussion, we set $\theta_0=0$ in the following content. Combining Eqs. (3), (1g), and (2), we can obtain the pore fluid pressure, the displacement of the solid $\boldsymbol{u}^{(\rm d)}$, the relative velocity of fluid-solid motion $\boldsymbol{w}^{(\rm d)}$, and the accompanied electric field $\boldsymbol{E}^{(\rm d)}$. However, the accompanied magnetic field $\boldsymbol{H}^{(\rm d)}=1/({\rm i}\omega\mu)\times\boldsymbol{E}=0$.

2.2.2. Reflection field in fluid-saturated porous medium

Outside the borehole, for the radiation conditions, the solutions of the reflection field are given by

$$\varphi_n^{(\rm r)}(r,\theta,z)=\int_{-\infty}^{+\infty}\sum_{n=0}^{\infty}\sum_{j=\rm pf,ps}A_n^jK_n(\eta_j r)\cos n\theta\,{\rm e}^{{\rm i}k_z z}{\rm d}k_z, \quad (4a)$$

$$\chi_n^{(\rm r)}(r,\theta,z)=\int_{-\infty}^{+\infty}\sum_{n=0}^{\infty}\sum_{j=\rm sh,te}A_n^jK_n(\eta_j r)\sin n\theta\,{\rm e}^{{\rm i}k_z z}{\rm d}k_z, \quad (4b)$$

$$\Gamma_n^{(\rm r)}(r,\theta,z)=\int_{-\infty}^{+\infty}\sum_{n=0}^{\infty}\sum_{j=\rm sv,tm}A_n^jK_n(\eta_j r)\cos n\theta\,{\rm e}^{{\rm i}k_z z}{\rm d}k_z. \quad (4c)$$

According to Eqs. (2) and (4), the basic vector fields $\boldsymbol{u}$, $\boldsymbol{w}$, and $\boldsymbol{E}$ can be obtained. Applying them to Eq. (1), all other quantities such as stress tensor, pore fluid pressure, and magnetic vector can also be deduced. The detailed expressions of these formulations can be found in Ref. [22].

So far, outside the borehole, the total fields including the incident field and reflect field can be induced.

2.3. Acoustic and electromagnetic fields inside the borehole

The acoustic pressure and the electromagnetic field inside the borehole are uncoupled.

2.3.1. Acoustic pressure inside the borehole

The displacement potential of borehole fluid can be written as[22]

$$\Phi(r,\theta,z)=\frac{1}{2\pi}\int_{-\infty}^{+\infty}\sum_{n=0}^{\infty}A_n^{\rm m}(k_z,\omega)I_n(\eta_{\rm f} r)\cos n\theta\,{\rm e}^{{\rm i}k_z z}{\rm d}k_z, \quad (5)$$

where A_n^m is the transmission coefficient. The radial component of the displacement field $u_r(r,\theta,z)$ and borehole fluid pressure $p(r,\theta,z)$ are obtained using $u_r=\partial\Phi/\partial r$ and $p=\omega^2\rho_{\rm f}\Phi$.

2.3.2. Electromagnetic field inside the borehole

When the electromagnetic field is relevant to angle, a separation variable approach is needed to deal with the components of the electric field on the radial non-homogeneous second-order partial differential equations. For convenience, we take the longitudinal component of electromagnetic field as auxiliary condition function, i.e.,

$$\begin{cases} E_z(r,\theta,z)=\dfrac{1}{2\pi}\displaystyle\int_{-\infty}^{+\infty}\sum_{n=0}^{\infty}A_n^{\rm e}I_n(\eta_{\rm e} r)\cos n\theta\,{\rm e}^{{\rm i}k_z z}{\rm d}k_z, \\ H_z(r,\theta,z)=\dfrac{1}{2\pi}\displaystyle\int_{-\infty}^{+\infty}\sum_{n=1}^{\infty}A_n^{\rm h}I_n(\eta_{\rm e} r)\sin n\theta\,{\rm e}^{{\rm i}k_z z}{\rm d}k_z, \end{cases} \quad (6)$$

where $\eta_{\rm e}^2=k_z^2-k_{\rm e}^2$, $k_{\rm e}^2=\omega^2\mu_{\rm e}\varepsilon_{\rm b}$, and $\varepsilon_{\rm b}=\varepsilon_{\rm f}+{\rm i}\sigma_{\rm f}/\omega$, with $\mu_{\rm e}$ being the magnetic permeability. Substituting Eq. (6) into Maxwell's equation, transverse field components are obtained, and detailed expressions of those formulations could be found in Ref. [22].

2.4. Boundary condition

The boundary conditions of seismoelectric waves for a cylindrical interface at the position $r=a$ between a fluid and a fluid-saturated formation are

$$\begin{cases} (u_r)_{\rm II}+(w_r)_{\rm II}=(U_r)_{\rm I}, & (p_{\rm f})_{\rm II}=(p)_{\rm I}, & (\tau_{\rm rr})_{\rm II}=(-p)_{\rm I}, \\ (\tau_{rz})_{\rm II}=0, & (\tau_{r\theta})_{\rm II}=0, & (E_\theta)_{\rm II}=(E_\theta)_{\rm I}, \\ (E_z)_{\rm II}=(E_z)_{\rm I}, & (H_\theta)_{\rm II}=(H_\theta)_{\rm I}, & (H_z)_{\rm II}=(H_z)_{\rm I}, \end{cases} \quad (7)$$

where subscripts I and II correspond to fluid of borehole and porous formation. The boundary equation may be written in the form of

$$M_{9\times 9}A_{9\times 1}=B_{9\times 1}, \qquad (8)$$

where

$$\boldsymbol{A}_{9\times1}=\left\{A_n^{\rm m},A_n^{\rm pf},A_{\rm n}^{\rm ps},A_n^{sh},A_n^{\rm te},A_n^{\rm sv},A_{\rm n}^{\rm tm},A_n^{\rm e},A_n^{\rm h}\right\}^{\rm T},$$
$$\boldsymbol{B}_{9\times1}=\{b_1,b_2,b_3,b_4,b_5,b_6,b_7,0,0\}^{\rm T},$$

and $\boldsymbol{B}_{9\times1}$ corresponds to the radiation field of acoustic source in fluid-saturated porous medium. The expressions are given by

$$\begin{aligned} b_1 &= \{(1+\alpha_j)\Theta_j[(n/r)I_n(\eta_j r)+\eta_j I_{n+1}(\eta_j r)]\}_{j=\rm pf}, \\ b_2 &= \{k_j^2(-M\alpha_j-C)[\Theta_j I_n(\eta_j r)]\}_{j=\rm pf}, \\ b_2 &= \{\Theta_j\{[-[H-2G+C\alpha_j]k_j^2+2G[(n^2-n)/r^2+\eta_j^2]] \\ &\quad \times I_n(\eta_j r)-2G(\eta_j/r)I_{n+1}(\eta_j r)\}\}_{j=\rm pf}, \\ b_4 &= \{-{\rm i}k_z 2\Theta_j[(n/r)I_n(\eta_j r)+\eta_j I_{n+1}(\eta_j r)]\}_{j=\rm pf}, \\ b_5 &= \{-\Theta_j[(2n(n-1)/r^2)I_n(\eta_j r) \\ &\quad +(2n/r)\eta_j I_{n+1}(\eta_j r)]\}_{j=\rm pf}, \\ b_6 &= \{-\Theta_j\beta_j(n/r)I_n(\eta_j r)\}_{j=\rm pf}, \\ b_7 &= \{\Theta_j{\rm i}\beta_j k_z I_n(\eta_j r)\}_{j=\rm pf}, \end{aligned}$$

where $\Theta_j=[\varepsilon_n/(2\pi)K_n(\eta_j r_0)\cos n\theta]_{j=\rm pf}$.

The complex matrices $M_{9\times9}$ can be found in Ref. [22].

3. Numerical results

In the space–time domain, the acoustic wave field and the electromagnetic field can be generally expressed as

$$F(r,\theta,z,t)=\frac{1}{2\pi}\int_{-\infty}^{+\infty}\Xi(r,\theta,z,\omega)F(\omega)\mathrm{e}^{-\mathrm{i}\omega t}\,\mathrm{d}\omega, \quad (9)$$

where Ξ can be p, E_z, E_r, E_θ, H_z, H_r, H_θ, etc.

The parameters in this paper are defined as: solid bulk modulus $K_\mathrm{s}=3.57\times10^{10}$ Pa; frame bulk modulus $K_\mathrm{b}=1.439\times10^{10}$ Pa; $G=1.399\times10^{10}$ Pa; fluid bulk modulus $K_\mathrm{f}=0.225\times10^{10}$ Pa; fluid viscosity $\eta=0.001$ Pa·s; tortuosity $\alpha_\infty=3$; porosity $\psi=0.21$; permeability $\kappa=3\times10^{-13}$ m^2; salinity $C_\mathrm{f}=0.01$ mol/L.

This study focuses on the acoustoelectric fields excited by the explosive point source located in the saturated porous medium. Especially for the condition that the centre frequency (f_0) is low and the distance (r_0) from the acoustic source to the axis of vertical borehole is far, it is easy to obtain valid data. It may be helpful in explaining cross-seismic data and has a potential significance in the actual oil exploration. In addition, microseisms are common in rocks ranging from tight sandstones and gas shales to carbonates and even volcanic, and at depths ranging from tens of meters to more than four thousand meters.[31] Data in the literature show that, typically, microseisms associated with a cross borehole have dominant frequencies extending from 200 Hz to approximately 1 kHz.

The condition of microseismic monitoring is also considered. In the first section, we discussed the effect of r_0 in the case of $f_0=1$ kHz.

When the distance changes gradually from $r_0=0.11$ m to $r_0=1$ m, the received acoustic wave field and electric field are shown in Fig. 2. Figure 2(a) shows that when $r_0=0.11$ m, we can find the distinct longitudinal wave packets, Stoneley wave packets, etc. In Fig. 2(b), the coseismic longitudinal wave packets, the coseismic Stoneley wave packets can also be found. With r_0 increasing, Stoneley wave packets, coseismic Stoneley wave packets, and so on all become less obvious. Especially when $r_0=1$ m, only the longitudinal wave packets and coseismic longitudinal wave packets can be observed in Figs. 2(a) and 2(b), respectively. One of the possible reasons for explaining the above phenomenon is that with r_0 increasing, the coupling effect between acoustic wave and borehole weakens. Therefore, the acoustic and electric fields we received are mainly determined by the incident longitudinal wave. That is to say, the reflection field is very weak. The above results also confirm that the seismoelectric conversion is induced on the fluid-saturated porous medium side of the borehole, not on the borehole fluid side.[9]

At the same time, in order to testify the validity of numerical full-waveform simulation method, we compare the results obtained in this paper with that using quasi-steady method proposed by Hu. Moreover, we find that there are no differences between the results from the two methods. For convenience, we will only show the results derived from the coupled method in this paper.

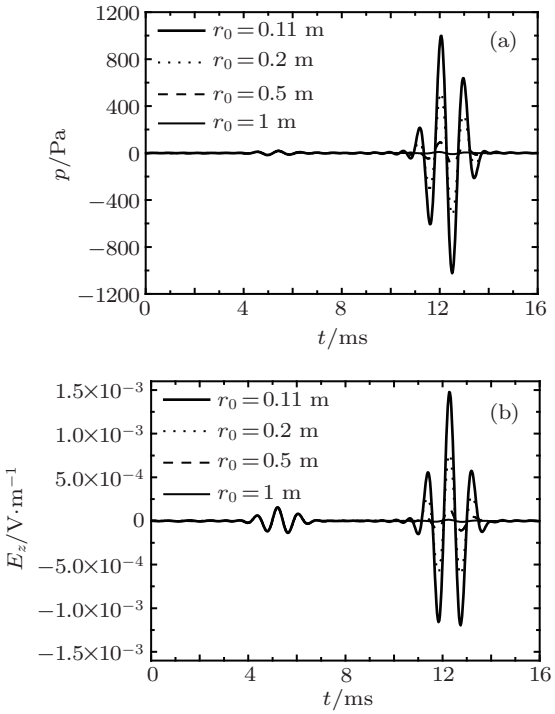


Fig. 2. Waveforms of (a) acoustic wave field and (b) electric field E_z with different values of r_0 $f_0=1000$ Hz, $r_\mathrm{re}=0.01$ m, $z=15$ m, and $\theta=0$.

Then, we pay our attention to obtain multipole acoustoelectric field in condition that r_0 is large and f_0 is low. The adopted parameters are: $r_0=50$ m, $f_0=100$ Hz, and $r_\mathrm{re}=0.01$ m. Now the coupling effect between the incident waves and borehole is weak. If we do not consider the borehole, we only receive acoustic pressure p, the displacements u_z and u_r, and the electrical fields E_z and E_r. However, duo to the existence of borehole, magnetic field H_θ can also be received inside the borehole. We can also use the magnetic information in the inverse problem as new magnetic sensors can be used in boreholes. The magnetic field is easier to invert than the electrical field as the magnetic permeability is constant and the electrical conductivity is not constant.[29]

Because the eccentric explosive source can be represented as superposition of multipole acoustic source. For one thing, we distinguish the monopole, dipole, quadrupole, and hexapole from multipole sources. Here we set $z=50$ m. Figure 3 shows that the received multipole acoustoelectric field in the borehole fluid is excited by the point source outside the borehole. Comparing the acoustic wave field with the electric field, if the acoustic pressure is 10^3 Pa, we can record the electric field on the order of 10^{-4} V. In Figs. 3(a)–3(d), we only observe the longitudinal wave packets obviously. The longitudinal waves are mainly excited and converted by monopole component, as shown in Figs. 3(a), 3(b), and 3(d). However, figure 3(c) shows that the longitudinal wave packets are mainly excited and converted by the dipole component in the electric field E_r.

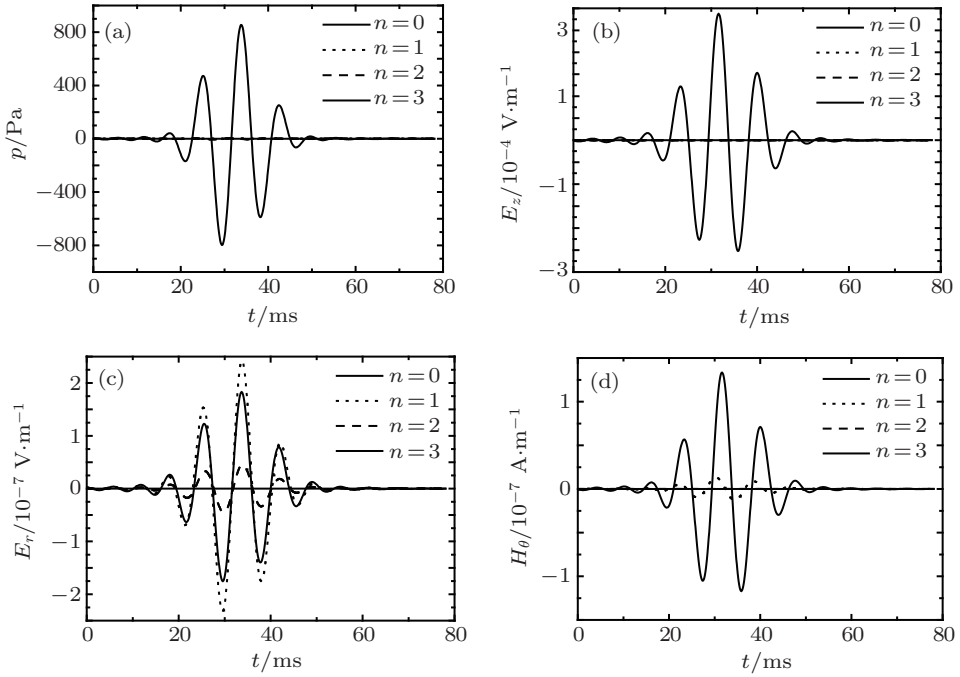


Fig. 3. An investigation for distinguishing (a) acoustic wave field p, (b) electric field E_z, (c) electric field E_r, and (d) magnetic field H_θ at $f_0 = 100$ Hz, $r_{\rm re} = 0.01$ m, $z = 50$ m, and $\theta = 0$.

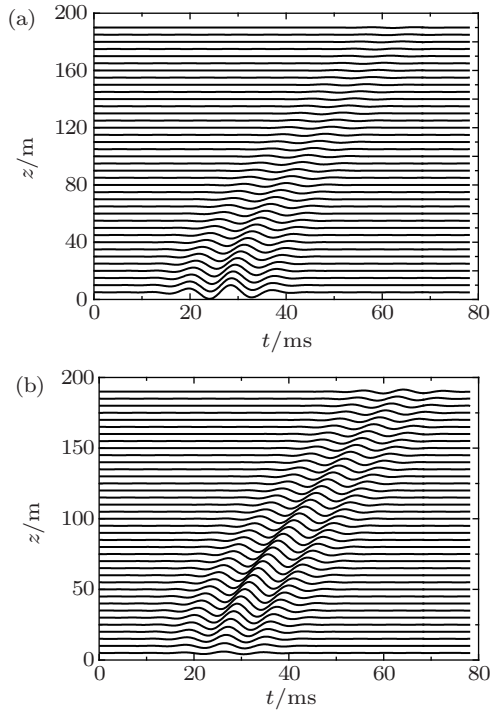


Fig. 4. The full wave (a) acoustic wave field and (b) electric field obtained by multichannel measurement. The number of channel is 38, and the other parameters are the same as those in Fig. 3.

Furthermore, we consider the influence of the receiving position along the axis of vertical borehole by multichannel receivers. Figure 4 shows the full wave contrast diagram of acoustoelectric field obtained by multichannel measurement. With the increase in the distance (z) from receivers to the origin of coordinate, the amplitude of longitudinal wave packets always attenuates in the acoustic pressure field p. However, in electric field E_z, the amplitude of longitudinal wave packets first increases, and then decreases. Figure 5 clearly depicts the position of the maximum acoustoelectric field.

The displacement potential function of a spherical wave can be described as $\varphi = Q\mathrm{e}^{\mathrm{i}kR}/R$. Therefore, in the cylindrical coordinate system, the axial component of displacement outside the borehole can be written as

$$|u_z| = \frac{Qz}{R^2}\sqrt{\left(k^2 + \frac{1}{R^2}\right)} = Q\sqrt{\frac{z^2}{(z^2+r^2)^2}\frac{\omega^2}{V_{\rm pf}^2} + \frac{z^2}{(z^2+r^2)^3}}.$$

When $r = z$, one can obtain the maximum values of u_z and E_z because the electric field E_z is accompanied by u_z in the porous formation outside the borehole according to Eq. (2). It should be noted that the electric field E_z is continuous at borehole wall, and u_z is not. Therefore, inside the borehole, at this moment, E_z also reaches a maximum value, and u_z does not. Just as shown in Fig. 5, when $z = 50$ m, the amplitude of the longitudinal wave reaches its maximum value in the electric field E_z (Fig. 5(a)). However, in Fig. 5(b) the maximum value of the displacement u_z is located at $z = 35$ m. Therefore, if we obtain the location of the maximum E_z at the borehole axis, we will be able to determine the distance from the acoustic source to the borehole axis.

If we estimate the position of acoustic source, we could use the electric field E_r or the displacement u_r. Figure 5 shows that the amplitudes of the electric field E_r and displacement u_r all monotonically decrease and their maximum amplitudes occur in $z = 0$ plane where the receiver is just located. When $z = 0$, we obtain the maximum amplitudes of electric field E_r

with different values of incident angle θ as shown in Fig. 6. It is easy to find that the electric field E_r is axisymmetric and the acoustic source is just located at the axis of symmetry.

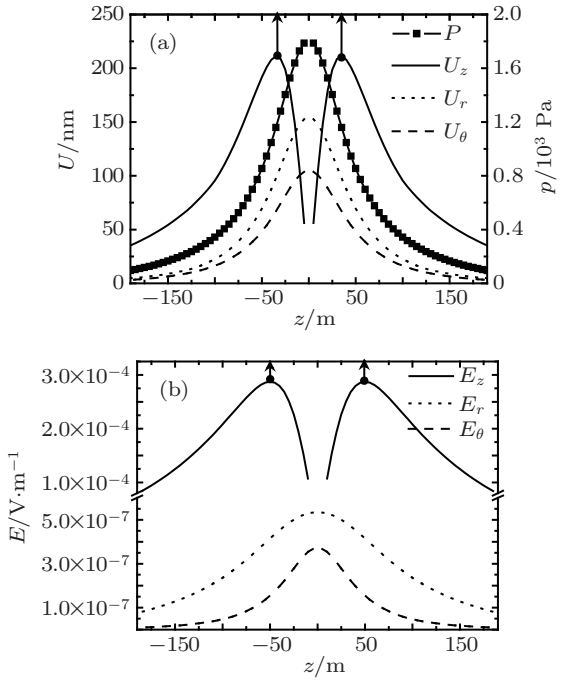


Fig. 5. The maximum amplitudes of (a) the acoustic wave field p and the displacement u, and (b) electric field E, obtained by multichannel measurement. The parameters are the same as those in Fig. 3.

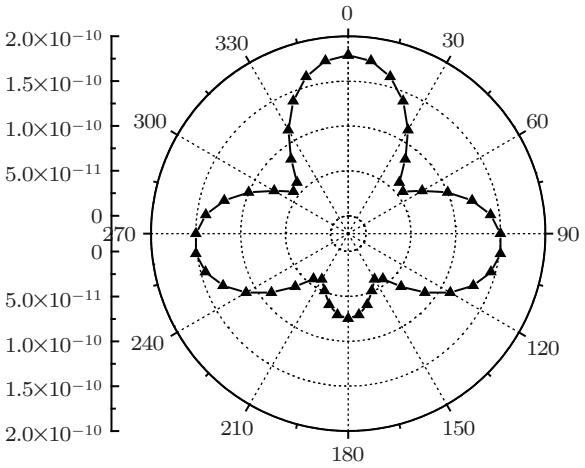


Fig. 6. Maximum amplitudes of electric field E_r with different values of θ when $z = 0$. The other parameters are the same as that in Fig. 3.

4. Conclusions

In this paper, we consider the acoustic and electric fields excited by the explosive point source outside of the borehole surrounded by the saturated porous medium based on Pride's theory. We present theoretical expressions for wave fields and analyze numerical results of the acoustic and electric fields based on both the coupled method and quasi-steady method. The algorithms in this paper to simulate seismoelectric wave propagation prove to be valid and efficient. Due to the existence of borehole, the electric fields and magnetic fields in the borehole are azimuthal. Inside the borehole, the three components of either electric field or magnetic field can be detected, and the radial electric field is mainly excited and converted by the dipole component. The magnetic field is easier to invert than the electrical field as the magnetic permeability is constant and the electrical conductivity is not constant. When the distance from the acoustic source to the axis of a borehole is large, the longitudinal and coseismic longitudinal wave packets dominate the acoustic and electric field, respectively. According to the location of the maximum axial component of electric field which is continuous at borehole wall, we will be able to determine the distance from the acoustic source to the borehole axis. The results of this paper may be significant for the seismoelectric effect to be used in microseisms and cross-hole measurements.

References

[1] Pride S R 1994 *Phys. Rev. B* **50** 15678
[2] Pride S R and Haartsen M W 1996 *J. Acoust. Soc. Am.* **100** 1301
[3] Zhu Z Y and Toksöz M N 2005 *Geophys.* **70** F45
[4] Bordes C, Jouniaux L, Dietrich M, Pozzi J P and Garambois S 2006 *Geophys. Res. Lett.* **33** L01302
[5] Bordes C, Jouniaux L, Garambois S, Dietrich M, Pozzi J P and Gaffet S 2008 *Geophys. J. Int.* **174** 489
[6] Haartsen M W and Pride S R 1997 *J. Geophys. Res.* **102** 24745
[7] Zhu Z Y, Haartsen M W and Toksöz M N 1999 *Geophys.* **64** 1349
[8] Zhu Z Y, Haartsen M W and Toksöz M N 2000 *J. Geophys. Res.* **105** 28055
[9] Zhu Z Y and Toksöz M N 2003 *Geophys.* **68** 1519
[10] Block G I and Harris J G 2006 *J. Geophys. Res.* **111** B01304
[11] Long L T and Rivers W K 1975 *Geophys.* **40** 233
[12] Butler K E, Russell R D, Kepic A W and Maxwell M 1996 *Geophys.* **61** 1769
[13] Mikhailov O V, Haartsen M W and Toksöz M N 1997 *Geophys.* **62** 97
[14] Beamish D 1999 *Geophys. J. Int.* **137** 231
[15] Garambois S and Dietrich M 2001 *Geophys.* **66** 1417
[16] Dupuis J C, Butler K E and Kepic A W 2007 *Geophys.* **72** A81
[17] Haines S S, Pride S R, Klemperer S L and Biondi B 2007 *Geophys.* **72** G9
[18] Revil A and Jardani A 2010 *Geophys. J. Int.* **180** 781
[19] Hu H S, Liu J Q, Wang H B and Wang K X 2003 *Chin. J. Geophys.* **46** 362
[20] Pain C C, Saunders, Worthington M H, Singer J M, Stuart-Bruges W, Mason G and Goddard A 2005 *Geophys. J. Int.* **160** 592
[21] Guan W, Hu H S and Chu Z T 2006 *Acta Phys. Sin.* **55** 0267 (in Chinese)
[22] Cui Z W 2004 *Theroretical and Numerical Study of Modified Biot's Models, Acoustoelectric Well Logging and Acoustic Logging While Drilling Excited by Multipole Acoustic Sources* (Ph.D thesis) (Changchun: Jilin University) (in Chinese)
[23] Cui Z W, Wang K X, Hu H S and Sun J G 2007 *Chin. Phys.* **16** 0746
[24] Zhu Z Y, Chi S H, Zhan X and Toksöz M N 2008 *Commun. Comput. Phys.* **3** 109
[25] Hunt C W and Wothington M H 2000 *Geophys. Res. Lett.* **27** 1315
[26] Mikhailov O V, Queen J H and Toksöz M N 2000 *Geophys.* **65** 1098
[27] Dupuis J C and Butler K E 2006 *Geophys. Res. Lett.* **33** L16301
[28] Araji A H, Revil A, Jardani A, Minsley B J and Karaoulis M 2012 *Geophys. J. Int.* **188** 1285
[29] Gao Y X and Hu H S 2010 *Geophys. J. Int.* **181** 873
[30] Hu H S and Gao Y X 2011 *J. Geophys. Res.* **116** B08302
[31] Warpinski N 2009 *JPT* **118537** 80